In Vivo Visualization of Cranial Nerve Pathways in Humans Using Diffusion-Based Tractography

Mojgan Hodaie, MD, MSc

Division of Neurosurgery,
University of Toronto and
Toronto Western Hospital,
Toronto, Canada

Jessica Quan, BSc

Faculty of Medicine,
Queen's University,
Kingston, Canada

David Qixiang Chen, BSc

Division of Neurosurgery,
University of Toronto and
Toronto Western Hospital,
Toronto, Canada

Reprint requests:
Mojgan Hodaie, MD, MSc,
University of Toronto,
4WW-443, 399 Bathurst Street,
Toronto, ON, Canada M5T 2S8.
E-mail: mojgan.hodaie@uhn.on.ca

Received, July 2, 2009.
Accepted, November 22, 2009.

OBJECTIVE: Diffusion-based tractography has emerged as a powerful technique for 3-dimensional tract reconstruction and imaging of white matter fibers; however, tractography of the cranial nerves has not been well studied. In particular, the feasibility of tractography of the individual cranial nerves has not been previously assessed.

METHODS: 3-Tesla magnetic resonance imaging scans, including anatomic magnetic resonance images and diffusion tensor images, were used for this study. Tractography of the cranial nerves was performed using 3D Slicer software. The reconstructed 3-dimensional tracts were overlaid onto anatomic images for determination of location and course of intracranial fibers.

RESULTS: Detailed tractography of the cranial nerves was obtained, although not all cranial nerves were imaged with similar anatomic fidelity. Some tracts were imaged in great detail (cranial nerves II, III, and V). Tractography of the optic apparatus allowed tracing from the optic nerve to the occipital lobe, including Meyer's loop. Trigeminal tractography allowed visualization of the gasserian ganglion as well as postganglionic fibers. Tractography of cranial nerve III shows the course of the fibers through the midbrain. Lower cranial nerves (cranial nerves IX, XI, and XII) could not be imaged well.

CONCLUSION: Tractography of the cranial nerves is feasible, although technical improvements are necessary to improve the tract reconstruction of the lower cranial nerves. Detailed assessment of anatomy and the ability of overlaying the tracts onto anatomic magnetic resonance imaging scans is essential, particularly in the posterior fossa, to ensure that the tracts have been reconstructed with anatomic fidelity.

KEY WORDS: Brainstem, Cranial nerves, Diffusion tensor imaging, Tractography, 3D Slicer

Neurosurgery 66:788-796, 2010 DOI: 10.1227/01.NEU.0000367613.09324.DA www.neurosurgery-online.com

The anatomic visualization of the cranial nerves (CNs) is of great interest in neurosurgery, from both diagnostic and surgical anatomy perspectives. Optimal visualization of the CNs has been carried out using a variety of magnetic resonance imaging (MRI) sequences such as fast imaging employing steady-state acquisition sequence and constructive interference in steady-state sequence, as well as higher-field MRI (3 T or higher).[1-4] These types of studies provide excellent visualization of CN structures in 2 dimensions; however, they lack adequate measures of tract continuity and integrity. Furthermore, the 3-dimensional relationship with other structures cannot be immediately derived from these images.

Recent advances in neuroimaging include the addition of diffusion tensor imaging (DTI) and tractography. This MRI-based image analysis technique allows reconstruction of white matter fiber tracts, based on the principle that diffusion of water molecules within white matter is not equal in all directions.[5] Rather, diffusion is maximal along the direction of the fiber tracts and is therefore anisotropic.[6] The technique of DTI assigns 3-dimensional vector fields, which are then reconstructed and represented pictorially. In this manner, a reconstructed model of the fiber tracts is obtained in a manner that is highly reproducible. The principles of this technique have been previously described,[6-9] as have the applications of this technique to the neurosurgical realm, including glioma surgery.[7,10-12] Furthermore, at least 1 method of neuronavigation that integrates DTI data (BrainLAB, Heimstetten, Germany) with conventional MRI is currently being used as part of intraoperative guidance.

ABBREVIATIONS: CN, cranial nerve; **DTI,** diffusion tensor imaging; **DWI**, diffusion-weighted imaging; **FA**, fractional anisotropy; **LGB**, lateral geniculate body; **MLF**, medial longitudinal fasciculus; **MRI**, magnetic resonance imaging; **ROI**, region of interest

Supplemental digital content is available for this article. Direct URL citations appear in the printed text and are provided in the HTML and PDF versions of this article on the journal's Web site (www.neurosurgery-online.com).

While the feasibility of tractography for delineation of large fiber bundles such as the corpus callosum and the corticospinal tract has been demonstrated,[13-16] its role in accurate delineation of small bundles remains to be studied. In general, small bundles are more difficult to image by lower-field MRI; they need smaller definitions of region of interest (ROI) or seed; and tract reconstruction is more difficult, particularly if the tracts are in the proximity of larger bundles. Tracking of small fiber bundles through regions where there is the possibility of crossing fibers has been an ongoing challenge.

We have been primarily interested in the role of tractography in delineating small fiber bundles in the brain. As part of this work, we addressed the feasibility of in vivo identification of the CNs and their pathways. The CNs consist of well-defined, small fiber bundles with known intra- and extracranial courses. They are therefore well-suited candidates for this study, particularly since tractography of these fibers would not generally interfere with crossing intracranial fibers. For this purpose, we used 3-T MRI scans from patients without structural lesions to determine (1) whether tractography can adequately reconstruct the course of the CNs (CNs II–XII); (2) what information tractography can provide beyond that obtained with 2-dimensional imaging; and (3) possible restrictions of this modality for imaging analysis.

PATIENTS AND METHODS

3-Tesla MRI scans of 4 patients who had been previously investigated primarily in preparation for functional neurosurgical procedures were chosen for this study after institutional Research Ethics Board approval was obtained. Review of anatomic MRI scans did not reveal any structural changes in the brainstem at the levels of interest. Attempts were made to reconstruct the course of CNs II to XII in each case.

Data Acquisition

A General Electric Signa 3-T MRI scanner (General Electric, Milwaukee, WI) was used to acquire all images. Both T1-weighted anatomic imaging scans and diffusion-weighted imaging (DWI) scans were obtained for each patient. The T1 scans were acquired as axial fast spoiled, gradient-recalled acquisition in steady state (slice thickness, 1 mm; slice spacing, 1 mm; repetition time, 8.0 milliseconds; echo time, 3.1 milliseconds). The DWI scans were acquired using an 8-channel head coil using DTI 25-directions array spatial sensitivity encoding technique, with echo planar/spin echo sequence (3-mm thickness; 55 slices; 1 baseline; spacing, 0 mm; echo time, 86.6 milliseconds; repetition time, 12 000 milliseconds; number of excitations, 1). The acquisition matrix size was 128 × 128, and the b-value was 1000 s/mm^2. The above sequence was used for all cases, after detailed study of the variables affecting the tract reconstruction, including number of directions, b-values, and repeats.

Image Processing

T1 anatomic and DWI scans were processed using 3D Slicer software (http://www.slicer.org, National Alliance for Medical Image Computing kit; versions 2.6 and 3.2α), using a Linux platform.[17] A baseline volume (B_0) and a DTI tensor volume (tensor map) were determined from the DWI scans using the least squares method. The baseline volume was overlaid onto the T1 anatomic scan using linear registration. The resulting transformation was also applied to the tensor volume so that any tracts obtained would align with the anatomic scan.

ROI Definition

ROIs were defined on the basis of the tensor volume at the area of the CN that could best be identified on 2-dimensional MRI scans. Seeding of the tracts was done by streamline tractography, with initial seed spacing of 0.5 mm, fractional anisotropy (FA) threshold of 0.2, and a curvature threshold of 0.8. FA values range from 0 to 1, with 1 representing maximal anisotropy along a perfect cylindrical shape. The tracts generated were examined. If any erroneous tracts were present, these were filtered using the "ROI Select NOT" operation. Multiple FA thresholds and seed spacings were assessed to ensure that a minimal number of erroneous tracts needed to be discarded. Assessment of the tracts and removal of erroneous tracts has been described previously.[18,19]

After the construction of the tracts, the images were superimposed on anatomic fast spoiled, gradient-recalled acquisition in steady state images for ease of visualization. Models of specific structures such as the eye and extraocular muscles were generated from manually defined volumes to visualize their relationships to the constructed tracts. Where a color-by-orientation map is represented, the convention of colors is used (red = right/left, green = anterior/posterior, blue = superior/inferior). The colors assigned to the CN tracts are arbitrary, unless specified as represented in functional anisotropy values. For ease of presentation, the 3-dimensional diffusion-based tracts have been overlaid on the closest 2-dimensional MRI slice that gives the closest representation of the location of the tract itself.

RESULTS

Seven of the 11 pairs of CNs studied could be imaged with ease, including the optic, oculomotor, trigeminal, abducens, facial/vestibular bundle, and vagus nerves. The olfactory nerve was not studied, given limited anatomic visualization. The results are detailed for each.

Before embarking on this study, we decided to ensure that our tractography method was strong enough to be used for the intended purpose. We therefore assessed and compared several different software tools for their ability to track fibers through a single voxel.[20] The voxel for the ROI was chosen as the area of the anterior commissure. We therefore observed (1) whether the fibers of the commissure could be tracked through a single voxel; (2) whether contaminating fibers were present, such that manual discarding of erroneous tracts was necessary; and (3) each of display of the tracts. The results are shown in Figure 1. Figure 1C displays the fibers of the anterior commissure tracked through a single voxel using 3D Slicer software. No contaminating fibers were encountered, and the tracks could be displayed with ease over diffusion images, anatomic images, or, in the case of the figure, mixed color-by-orientation/anatomic images. Having been satisfied with this technique, we applied the method to the visualization of the tracts of the CNs.

Optic Nerve

Tractography of the optic nerve included segments spanning the prechiasmatic portion, chiasm, retrochiasmatic tract, and

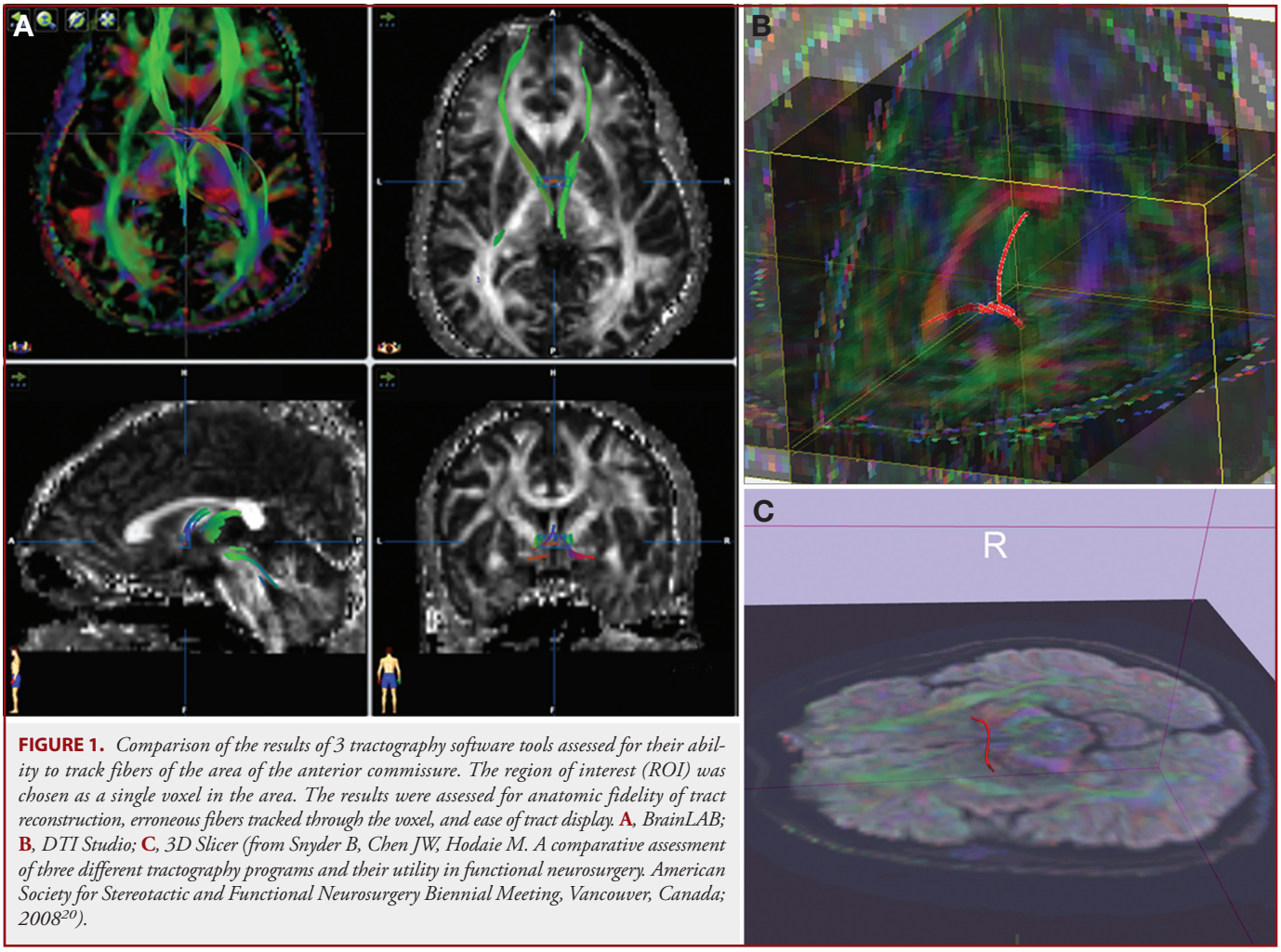

FIGURE 1. *Comparison of the results of 3 tractography software tools assessed for their ability to track fibers of the area of the anterior commissure. The region of interest (ROI) was chosen as a single voxel in the area. The results were assessed for anatomic fidelity of tract reconstruction, erroneous fibers tracked through the voxel, and ease of tract display.* **A**, *BrainLAB;* **B**, *DTI Studio;* **C**, *3D Slicer (from Snyder B, Chen JW, Hodaie M. A comparative assessment of three different tractography programs and their utility in functional neurosurgery. American Society for Stereotactic and Functional Neurosurgery Biennial Meeting, Vancouver, Canada; 2008[20]).*

optic radiation. Figure 2 shows the reconstructed tracts, including the prechiasmatic portion of the optic nerve, as well as the chiasm and the optic tract, up to the optic radiation and lateral geniculate body (LGB). This was obtained with seeds placed over the prechiasmatic portion of the optic nerve. As the fibers exit the LGB, tract interruption is seen at that point, probably because of the angle of the fibers exiting the LGB. A second seed was placed in the LGB area, after which fibers between this seed and the occipital lobe were selected. This allowed the reconstruction of fibers of the optic radiation, including Meyer's loop (Fig. 3), which can be clearly seen wrapping around the temporal horn of the lateral ventricle on its course toward the occipital lobe (Fig. 1, Supplemental Digital Content 1, http://links.lww.com/NEU/A291).

We elected to determine the degree of detail that could be ascertained for specific portions of the visual system. For this, we studied the relationship between the optic radiation tracts near the splenium of the corpus callosum (Fig. 4). The relationship between the fibers of the tapetum and the optic radiation in that area has been previously described.[21] Figure 4B shows a magnified image of the reconstructed optic radiation tracts at the splenium of the corpus callosum. The superior/inferior course of the tapetum fibers (represented in blue) can be seen clearly coursing between the wall of the lateral ventricle and the corona radiata (coursing anterior/posteriorly, in green), where the optic radiation fibers lie. Farther distally, the tracts reach the occipital lobe and can be traced nearly to the cortex, around the banks of the calcarine fissure (Fig. 2; Fig. 1, Supplemental Digital Content 1, http://links.lww.com/NEU/A291).

Oculomotor Nerve

The seed for the oculomotor nerve (CN III) was placed in the cisternal segment, where the nerve can best be visualized on anatomic images. A long course of CN III could be reconstructed, including a segment of its course through the brainstem. Distally, the course of CN III can be followed into what appears to be the cavernous sinus, while proximally, the fibers appear to angle upward and then descend into the brainstem. Evaluation of the position of the

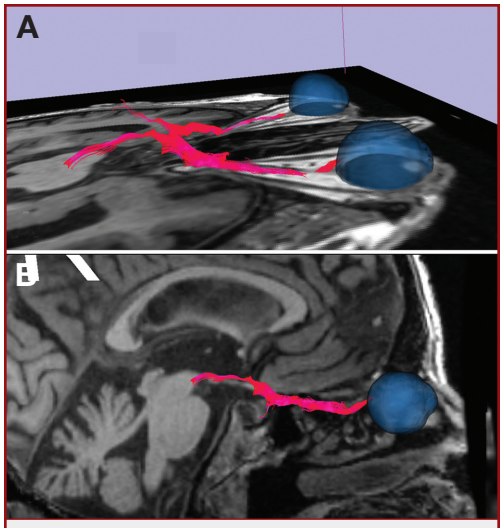

FIGURE 2. *Three-dimensional tract reconstruction for the optic apparatus, overlaid onto anatomic 3-T magnetic resonance imaging (MRI) slices.* **A**, *the optic nerve, chiasm, and optic tract. The globe has been outlined in blue as a separate volume. The angle of the chiasm compared with the optic nerve can be visualized.* **B**, *the same structures overlaid onto sagittal MRI sequences. (Please see also Supplemental Digital Content 1, Figure 1, a 3-dimensional representation of the optic chiasm, optic radiation, and Meyer's loop http://links.lww.com/NEU/A291.)*

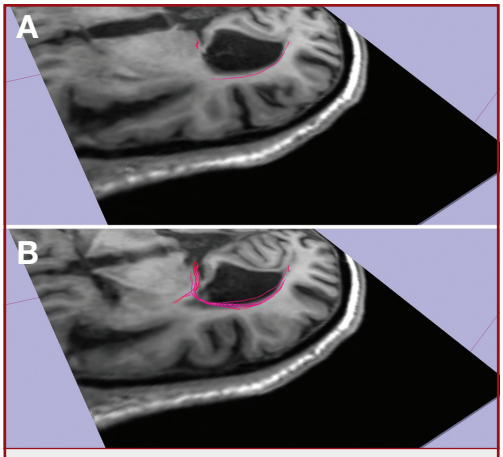

FIGURE 3. *Three-dimensional tract reconstruction for the optic apparatus with outlining tracts between the lateral geniculate body and occipital lobe.* **A** *and* **B**, *anatomic slices with overlaid temporal optic radiation fibers. Fibers delineating Meyer's loop can be visualized. The temporal fibers can be eventually traced onto the occipital lobe. (Please see also Supplemental Digital Content 1, Figure 1, a 3-dimensional representation of the optic chiasm, optic radiation, and Meyer's loop http://links.lww.com/NEU/A291.)*

descending tracts suggests that tractography permits visualization of CN III fibers as they appear to enter the area of the medial longitudinal fasciculus (MLF) (Figs. 5 and 6; Fig. 2, Supplemental Digital Content 2, http://links.lww.com/NEU/A292).

Trigeminal Nerve

The most robust reconstruction of the CNs corresponded to the trigeminal nerve. Distally, the fibers could be traced to the gasserian ganglion and beyond, identifying distal branches. The pattern of arrangement of the trigeminal branches arising from the gasserian ganglion could be easily observed. Proximally, at the nerve root entry zone, the fibers of CN V are likely mixed with tracts of the much larger, contiguous cerebellar peduncles, and interpretation of the course of CN V proximally is therefore compromised (Fig. *7*, A and B; Fig. 3, Supplemental Digital Content 3, http://links.lww.com/NEU/A293).

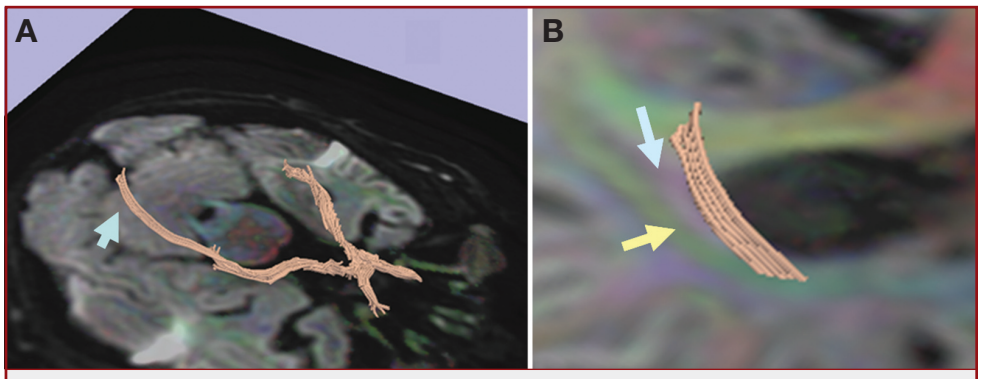

FIGURE 4. *Three-dimensional representation of the visual pathways, reconstructed from the optic nerve to distal fibers of the optic radiation and not including Meyer's loop. The 3-dimensional fibers are overlaid onto a midpontine axial MRI slice depicted in color-by-orientation mode.* **A**, *given that the tracts are represented in 3 dimensions, the fibers (arrow) are located in the parietal lobe. These fibers are located in the corona radiata (magnified in* **B**). **B**, *the location of the fibers of the optic radiation in the corona radiata. It can be seen that the reconstructed optic radiation fibers course along a green tract, which, by tractography convention, represents anterior/posterior directionality (yellow arrow). Medially and adjacent to it, with a location between these fibers and the ventricular wall, a tract shown in blue, based on diffusion tensor imaging convention (superior/inferior directionality), can be visualized. This tract likely corresponds to the fibers of the tapetum (blue arrow).*

Abducens Nerve

Tract reconstruction for the abducens nerve (CN VI) delineated primarily the course of its cisternal portion (Fig. 7C). No reconstructed tracts could be visualized within the substance of the brainstem. The course of the abducens nerve in its cisternal segment follows directly superiorly and rostrally, until its entrance into Dorello's canal. This is in keeping with previously published MRI studies of CN VI.[22,23]

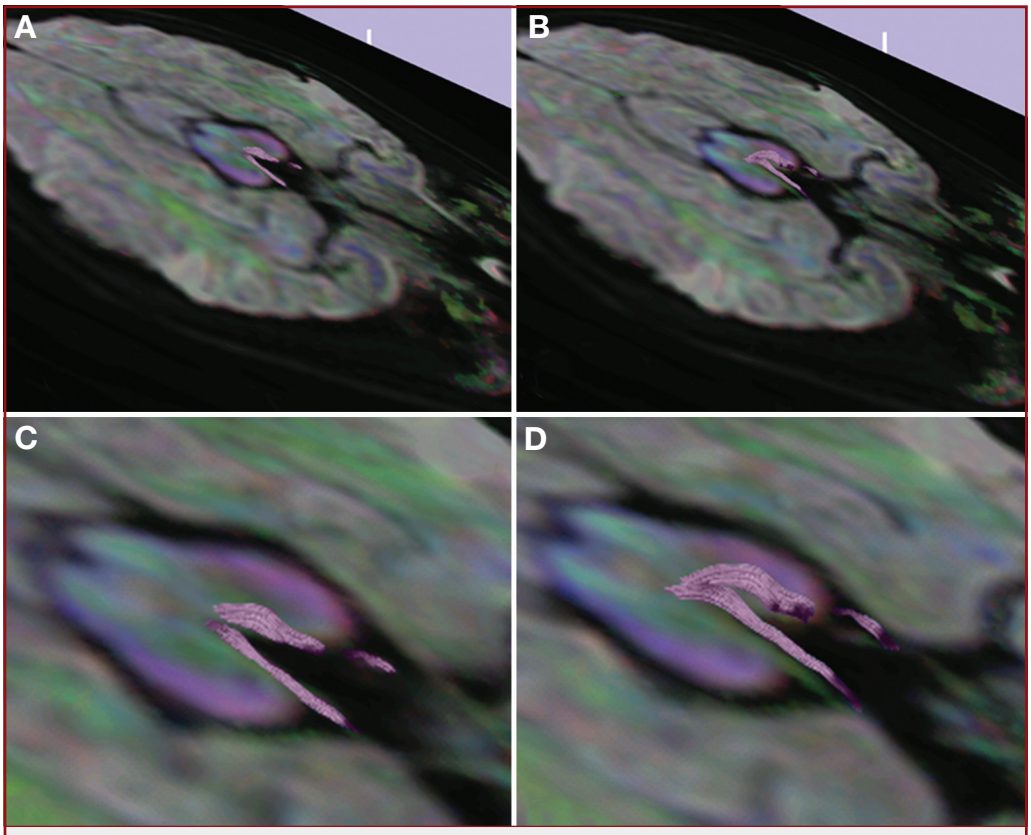

FIGURE 5. *Three-dimensional representation of the oculomotor fibers (cranial nerve III) onto mixed anatomic/color-by-orientation MRI slices. The oculomotor fibers are seen exiting the midbrain.* **C** *and* **D**, *magnified images of* **A** *and* **B**, *respectively. Slight flaring of the fibers is seen as these approach the nucleus within the substance of the midbrain.*

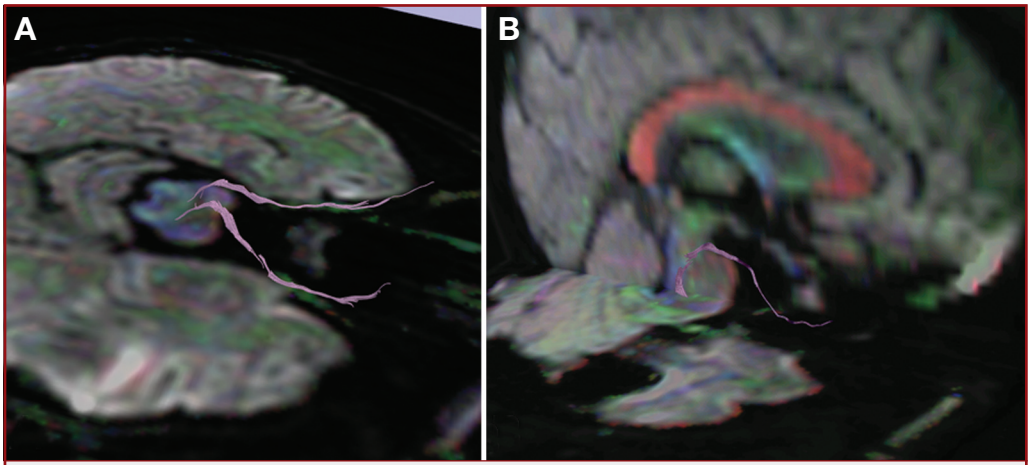

FIGURE 6. *Intra- and extracranial course of cranial nerve III, depicted onto mixed anatomic/color-by-orientation MRI slices. Images are overlaid onto axial MRI slices (*A*) and sagittal MRI slices (*B*). The intracranial course takes a sharp angle, after which the fibers appear to enter the medial longitudinal fasciculus. The large commissural fibers of the corpus callosum (red) and fornix (blue) can be easily visualized on the sagittal slices. (Please see also Supplementary Digital Content 2, Figure 2, a 3-dimensional representation of the oculomotor nerves.)*

Facial/Vestibular Complex

Tractography of the facial (CN VII) and vestibular-cochlear/auditory (CN VIII) bundle showed mainly the cisternal segment of the nerves extending to the internal auditory meatus (Fig. 8). The nerves were seen to travel in close proximity to each other and were not easily differentiated. Visualization of these nerves entering the brainstem was minimal and often mixed with larger fibers of the cerebellar peduncles. Seeds were placed at the area of the internal auditory meatus.

Lower Cranial Nerves

The seeds used to model the vagus (CN X) nerve were placed at the anterior aspect of the medulla on a coronal section of the tensor volume to reconstruct the course of the vagus nerve as it exits the brainstem. Only the cisternal portion of the nerve could be adequately reconstructed (Fig. 7D).

Recognition and localization of the trochlear (IV), glossopharyngeal (CN IX), accessory (CN XI), and hypoglossal (CN XII) nerves on the tensor volumes was technically challenging, probably as a result of magnetic distortion or signal-to-noise ratio. Thus, the corresponding tracts for these nerves were not reconstructed.

DTI Parameters

Parameters including number of fibers per ROI, number of fibers per voxel (fiber density), and FA values could be calculated. A sample calculation for the cisternal portion of the trigeminal nerve is presented in Table 1.

DISCUSSION

DTI has proved to be a powerful technique in neuroimag-

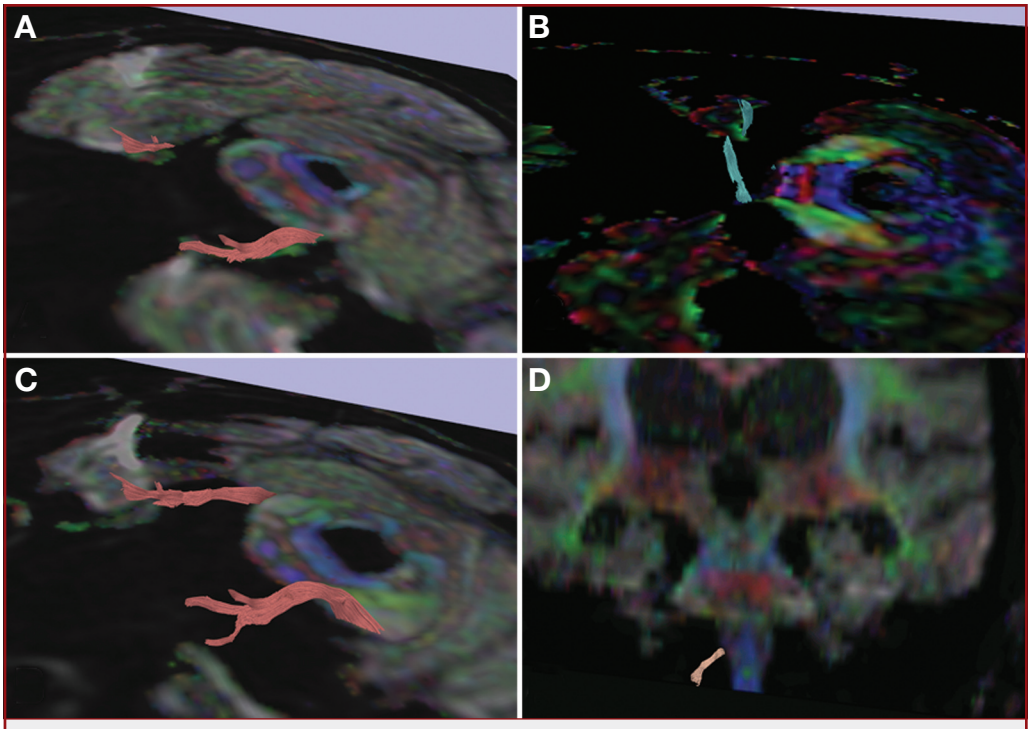

FIGURE 7. *Three-dimensional tract representation for the trigeminal (**A** and **B**), abducens (**C**), and vagus nerves (**D**), all overlaid onto color-by-orientation maps. The robust reconstruction of the trigeminal fibers can be seen, including the gasserian ganglion and distal branches. Proximally, the trigeminal fibers appear to mix with the fibers of the peduncles. (Please see also Supplementary Digital Content 3, Figure 3, a 3-dimensional representation of the trigeminal nerves.)*

ing, enhancing our ability to determine the detailed course of white matter fibers. The purpose of the present study was to assess whether this technique could be used to accurately reconstruct the course of CN fibers, including those in the posterior fossa, followed by a review of some of the benefits and technical challenges.

Although attempts were made to reconstruct the tracts of CNs II to XII in each case, we found that CNs II, III, and V showed the best degree of fiber reconstruction, with robust visualization of the optic nerve, tract, and radiation. For CN III, significant detail was seen, including its course within the brainstem, presumably into the MLF, and distally toward the cavernous sinus. Likewise, the reconstructed fibers of CN V were seen with great fidelity, tracking well into the distal trigeminal branches, beyond the gasserian ganglion. Visualization of the facial/vestibulocochlear complex extending into the auditory meatus was also possible, although further detail could not be discerned. Tractographic descriptions of the CNs, including delineation of the gasserian ganglion with its postganglionic branches, the oculomotor nerve and its course through the brainstem, and the tracts of the abducens nerve have not been previously reported.

In addition to a pictorial display of the tracts, tractography allows information on specific parameters, including FA and number of fibers per voxel (fiber density). A sample set of values for 3 ROIs of the trigeminal nerve are displayed in Table 1. DTI parameters can relay information regarding the microstructure of the nerve.[24,25] These parameters can be modified by axonal properties, including demyelination, inflammation, and diameter of the axons. There is increasing interest in the study of these parameters and how they can be affected by various disease states.[26]

We observed that 3D Slicer software had the ability to accurately reconstruct CN fibers deep into the brainstem and, in the case of the optic nerve, into the brain parenchyma itself. Both the optic radiation and Meyer's loop were easily modeled with tractography, with a surprising level of detail. This is apparent also in the visualization of the optic radiation in the corona radiata and its relationship with the fibers of the tapetum and ventricular wall (Fig. 4B). Furthermore, the extension of the oculomotor nerve into the brainstem and its connections with the MLF were also modeled (Fig. 6B). This suggests that DTI has the ability to visualize a continuum between the CNs and their central connections. In relation to possible applications such as preoperative planning, it may be possible to use DTI to investigate the structural integrity of not only the CNs themselves, but also their brainstem connections.[27,28] Previous studies have been published outlining Meyer's loop.[19,29] We attempted to outline the course of the optic nerve and radiation; however, it was not possible to do this using a single seed, likely because of the significant bend that occurs at the level of the lateral geniculate nucleus.

Despite the advances in diffusion-based tractography, some key issues remain. One of the ongoing challenges of tractography has been adequate tract reconstruction of small fiber bundles in the brain, and, in particular, in areas where larger, more robust bundles may also course. As seen in our CN models, nerve fibers exiting from the level of the pons were often confounded by the larger fiber bundles of the peduncles. This was seen for the trigeminal as well as the facial/vestibular-cochlear complex. Fiber tracks extending into the brainstem of these 3 CNs could not be reliably modeled without mixing with fibers of the peduncles. More recently, techniques using Q-ball tensor fields and diffusion spectral imaging are showing promise in accurately distinguishing crossing fibers.[30,31]

We would like to emphasize that one of the major problems with application of tractography technology to neurosurgery is the quality of the images over which the tracts are displayed. In fact,

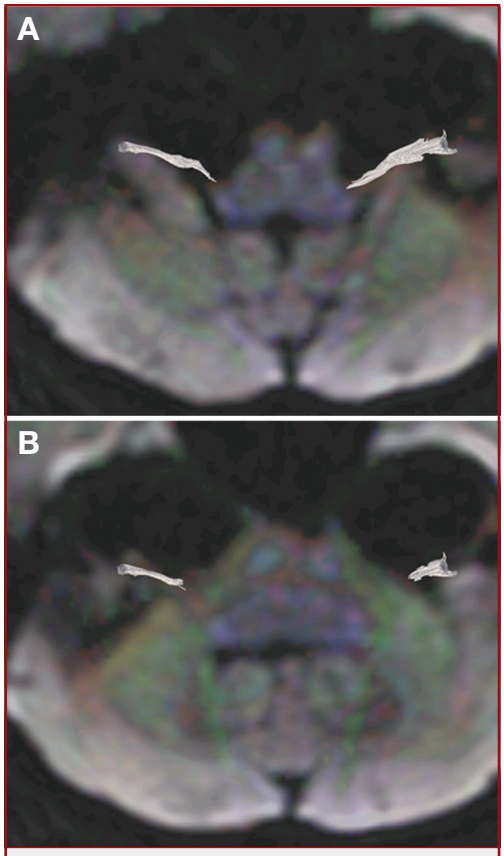

FIGURE 8. *Three-dimensional representation of the facial/vestibular complex, overlaid onto mixed anatomic/color-by-orientation MRI slices. Only the cisternal component of the fibers could be traced.*

TABLE 1. Example of Statistical Data Obtained From Selected Regions of Interest[a]

ROI No.	Fibers/ROI	Density (Fiber/Voxel)	FA Value
1	148	49.333	0.362
2	152	50.667	0.449
3	155	51.667	0.350
Average		50.556 ± 1.171	0.387 ± 0.054

[a] ROI, region of interest; FA, fractional anisotropy. Three ROIs were selected along the midcisternal portion of the trigeminal nerve. For each, fibers per ROI, fiber density, and FA values can be calculated.

previous studies have typically displayed tracts onto diffusion images, making visualization of the anatomy underlying the tract difficult to assess.[26,32-34] Large tracts, such as the corticospinal tract, can still be visualized well under these settings[12,35]; however, when small fibers are displayed, detailed anatomic assessment is necessary.[32,36,37] Therefore, in our study, we found the ability to display the tracts onto anatomic images to be a significant advantage. We would suggest, therefore, that without the ability to overlay the tracts onto anatomic images, the use of tractography for small fiber bundles in the brain would be highly limited.

The resolution of the DTI scans significantly limited our ability to visualize some of the smaller and more diffuse nerve bundles, along with the more distal nerve fibers. Despite being a relatively large bundle fiber, the vagus nerve fibers exiting the brainstem are very thin and diffuse. This dispersed orientation of thin fibers is likely to play a role in making the tensor information in this region relatively unreliable and, thus, difficult to track using DTI. Similarly, the glossopharyngeal nerve also takes on a dispersed pattern at the exit site of the brainstem. To improve the resolution of DTI scans requires smaller slice thicknesses, which relates to a hardware limitation of the scanner itself. However, other researchers have been investigating innovative methods of improving resolution using methods of MRI reconstruction and stacking of multiple scans.[38] Magnetic field distortions and lack of signal can also influence the poor resolution in the lower brainstem.

The proximity of the CNs to surrounding bony structures increases with caudal descent toward the medulla and the foramen magnum. It is possible that it is the interference from bony signal from the cranial base that impedes adequate tract reconstruction of the lower CNs. This was seen in both the cavernous sinus, as the oculomotor nerve exited the cranium, and in the lower CNs, as these are close to the base of the cranium and the foramen magnum.

Although this technical capability for reconstruction of the CN tracts is encouraging, we recognize that interpatient variability and the presence of pathology/degenerative changes may affect the results of tracking. Furthermore, these current methods are also subject to interinvestigator variability with respect to the selection of ROI locations. A method that has been suggested to overcome the interinvestigator variability is the use of a template of ROIs.[31] While this method may help reduce variability in terms of selection of ROIs, it may further limit the accuracy of visualizing small fiber bundles.

With the ongoing technical improvements in this mode of imaging, we foresee that tractography will become more integrated in the neurosurgical arena, with applications ranging from assessment of lesions in the cerebellopontine angle to surgical targeting in functional neurosurgery procedures.

CONCLUSIONS

Tractography is a feasible method of imaging of the CNs. Considerable detail in the fine structure of the CNs can be seen, including intracranial courses for CN II, CN III, and the distal branches of CN V. Factors that affect ease of tractography include the size of the CN bundle as well as the position of the CNs in the neuraxis, with consequent difficulty of imaging of the lower CNs. The ability of tractography software to allow the selection of very small seeds as well as overlaying of the images onto anatomic MRI slices is crucial for the interpretation of the results.

Disclosure

The authors have no personal financial or institutional interest in any of the drugs, materials, or devices described in this article.

REFERENCES

1. Everton KL, Rassner UA, Osborn AG, Harnsberger HR. The oculomotor cistern: anatomy and high-resolution imaging. *AJNR Am J Neuroradiol.* 2008;29(7):1344-1348.
2. Kakizawa Y, Seguchi T, Kodama K, et al. Anatomical study of the trigeminal and facial cranial nerves with the aid of 3.0-Tesla magnetic resonance imaging. *J Neurosurg.* 2008;108(3):483-490.
3. Nagae-Poetscher LM, Jiang H, Wakana S, Golay X, van Zijl PC, Mori S. High-resolution diffusion tensor imaging of the brain stem at 3 T. *AJNR Am J Neuroradiol.* 2004;25(8):1325-1330.
4. Naganawa S, Koshikawa T, Fukatsu H, Ishigaki T, Fukuta T. MR cisternography of the cerebellopontine angle: comparison of three-dimensional fast asymmetrical spin-echo and three-dimensional constructive interference in the steady-state sequences. *AJNR Am J Neuroradiol.* 2001;22(6):1179-1185.
5. Beaulieu C. The basis of anisotropic water diffusion in the nervous system—a technical review. *NMR Biomed.* 2002;15(7-8):435-455.
6. Mori S, van Zijl PC. Fiber tracking: principles and strategies—a technical review. *NMR Biomed.* 2002;15(7-8):468-480.
7. Chen X, Weigel D, Ganslandt O, Buchfelder M, Nimsky C. Diffusion tensor imaging and white matter tractography in patients with brainstem lesions. *Acta Neurochir (Wien).* 2007;149(11):1117-1131.
8. Ciccarelli O, Catani M, Johansen-Berg H, Clark C, Thompson A. Diffusion-based tractography in neurological disorders: concepts, applications, and future developments. *Lancet Neurol.* 2008;7(8):715-727.
9. Mori S, Frederiksen K, van Zijl PC, et al. Brain white matter anatomy of tumor patients evaluated with diffusion tensor imaging. *Ann Neurol.* 2002;51(3):377-380.
10. Keles GE, Berger MS. Advances in neurosurgical technique in the current management of brain tumors. *Semin Oncol.* 2004;31(5):659-665.
11. Nimsky C, Ganslandt O, Hastreiter P, et al. Preoperative and intraoperative diffusion tensor imaging-based fiber tracking in glioma surgery. *Neurosurgery.* 2005;56(1):130-138.
12. Nimsky C, Ganslandt O, Merhof D, Sorensen AG, Fahlbusch R. Intraoperative visualization of the pyramidal tract by diffusion-tensor-imaging-based fiber tracking. *Neuroimage.* 2006;30(4):1219-1229.
13. Catani M, Thiebaut de Schotten M. A diffusion tensor imaging tractography atlas for virtual in vivo dissections. *Cortex.* 2008;44(8):1105-1132.
14. Kamada K, Sawamura Y, Takeuchi F, al. Functional identification of the primary motor area by corticospinal tractography. *Neurosurgery.* 2007;61(1 Suppl):166-177.
15. Kamada K, Todo T, Masutani Y, et al. Visualization of the frontotemporal language fibers by tractography combined with functional magnetic resonance imaging and magnetoencephalography. *J Neurosurg.* 2007;106(1):90-98.
16. Muthusamy KA, Aravamuthan BR, Kringelbach ML, et al. Connectivity of the human pedunculopontine nucleus region and diffusion tensor imaging in surgical targeting. *J Neurosurg.* 2007;107(4):814-820.
17. Pieper S, Halle M, Kikinis R. 3D Slicer. Proceedings of the 1st IEEE international symposium on biomedical imaging: from nano to macro. 2004;1:632-635.
18. Techavipoo U, Okai AF, Lackey J, et al. Toward a practical protocol for human optic nerve DTI with EPI geometric distortion correction. *J Magn Reson Imaging.* 2009;30(4):699-707.
19. Yogarajah M, Focke NK, Bonelli S, et al. Defining Meyer's loop-temporal lobe resections, visual field deficits and diffusion tensor tractography. *Brain.* 2009;132(Pt 6):1656-1668.
20. Snyder B, Chen JW, Hodaie M. A comparative assessment of three different tractography programs and their utility in functional neurosurgery. American Society for Stereotactic and Functional Neurosurgery Biennial Meeting, Vancouver, Canada; 2008.
21. Peltier J, Travers N, Destrieux C, Velut S. Optic radiations: a microsurgical anatomical study. *J Neurosurg.* 2006;105(2):294-300.
22. Eisenkraft B, Ortiz AO. Imaging evaluation of cranial nerves 3, 4, and 6. *Semin Ultrasound CT MR.* 2001;22(6):488-501.
23. Ono K, Arai H, Endo T, et al. Detailed MR imaging anatomy of the abducent nerve: evagination of CSF into Dorello canal. *AJNR Am J Neuroradiol.* 2004;25(4):623-626.
24. Boorman ED, O'Shea J, Sebastian C, Rushworth MF, Johansen-Berg H. Individual differences in white-matter microstructure reflect variation in functional connectivity during choice. *Curr Biol.* 2007;17(16):1426-1431.
25. Nucifora PG, Verma R, Lee SK, Melhem ER. Diffusion-tensor MR imaging and tractography: exploring brain microstructure and connectivity. *Radiology.* 2007;245(2):367-384.
26. Kolappan M, Henderson AP, Jenkins TM, et al. Assessing structure and function of the afferent visual pathway in multiple sclerosis and associated optic neuritis. *J Neurol.* 2009;256(3):305-319.
27. Clark CA, Barrick TR, Murphy MM, Bell BA. White matter fiber tracking in patients with space-occupying lesions of the brain: a new technique for neurosurgical planning? *Neuroimage.* 2003;20(3):1601-1608.
28. Stadlbauer A, Nimsky C, Gruber S, et al. Changes in fiber integrity, diffusivity, and metabolism of the pyramidal tract adjacent to gliomas: a quantitative diffusion tensor fiber tracking and MR spectroscopic imaging study. *AJNR Am J Neuroradiol.* 2007;28(3):462-469.
29. Sherbondy AJ, Dougherty RF, Napel S, Wandell BA. Identifying the human optic radiation using diffusion imaging and fiber tractography. *J Vis.* 2008;8(10):12. 1-11.
30. Perrin M, Poupon C, Cointepas Y, et al. Fiber tracking in Q-ball fields using regularized particle trajectories. *Inf Process Med Imaging.* 2005;19:52-63.
31. Wedeen VJ, Wang RP, Schmahmann JD, et al. Diffusion spectrum magnetic resonance imaging (DSI) tractography of crossing fibers. *Neuroimage.* 2008;41(4):1267-1277.
32. Kabasawa H, Masutani Y, Aoki S, et al. 3T PROPELLER diffusion tensor fiber tractography: a feasibility study for cranial nerve fiber tracking. *Radiat Med.* 2007;25(9):462-466.
33. Mamata H, Mamata Y, Westin CF, et al. High-resolution line scan diffusion tensor MR imaging of white matter fiber tract anatomy. *AJNR Am J Neuroradiol.* 2002;23(1):67-75.
34. Taoka T, Hirabayashi H, Nakagawa H, et al. Displacement of the facial nerve course by vestibular schwannoma: preoperative visualization using diffusion tensor tractography. *J Magn Reson Imaging.* 2006;24(5):1005-1010.
35. Ng WH, Cheong DL, Khu KJ, Venkatesh G, Ng YK, Lim CC. Diffusion tensor tractography: corticospinal tract fiber reduction is associated with temporary hemiparesis in benign extracerebral lesions. *Neurosurgery.* 2008;63(3):452-459.
36. Yamada K, Shiga K, Kizu O, et al. Oculomotor nerve palsy evaluated by diffusion-tensor tractography. *Neuroradiology.* 2006;48(6):434-437.
37. Yamamoto A, Miki Y, Urayama S, et al. Diffusion tensor fiber tractography of the optic radiation: analysis with 6-, 12-, 40-, and 81-directional motion-probing gradients, a preliminary study. *AJNR Am J Neuroradiol.* 2007;28(1):92-96.
38. Shilling R, Robbie T, Bailloeul T, Mewes K, Mersereau R, Brummer M. A super-resolution framework for 3-D high resolution and high contrast imaging using 2-D multi-slice MRI. *IEEE Trans Med Imaging.* 2008;28(5):633-644.

Acknowledgment

We thank Andres M. Lozano, MD, for his helpful comments on this study.

Supplemental digital content *is available for this article. Direct URL citations appear in the printed text and are provided in the HTML and PDF versions of this article on the journal's Web site (www.neurosurgery-online.com).*

COMMENTS

The authors describe their experience with the use of 3-T MRI, diffusion tensor imaging, and tractography to create 3D reconstructions of cranial nerve fibers. Diffusion tensor imaging is a powerful pre- and intraoperative tool for visualizing large white matter tracts during neurosurgical procedures; however, the reconstruction of small fiber bundles with this technique has been difficult. Although excellent images of cranial nerves, including the lower cranial nerves and adjacent structures, have previously been obtained with various MRI modalities, including fast imaging employing steady-state acquisition, construction interference steady-state, and time-of-flight magnetic resonance angiography sequences, the authors present an expanded diffusion-based method for reconstruct-

ing small fiber tracts and evaluating tract continuity and integrity. In this report, images from 4 patients without structural abnormalities were used to attempt 3D reconstruction of the 12 pairs of cranial nerves, with success achieved in highly detailed images of cranial nerves II, III, and V. Incomplete images of cranial nerves VI, VII, VIII, and X, showing only the cisternal segments, were obtained; cranial nerves IV, IX, XI, and XII could not be imaged well because of extensive artifact and interference. Nonetheless, the 3D images created by the tractography of II, III, and V are impressive and represent a promising sign of the information that this technology can provide as it evolves. To further elucidate the clinical applications for this technology, further studies should include 3D small fiber tractography in patients with structural lesions, as well as techniques for reducing large fiber tract and bony interference.

Rasha S. Germain
Robert F. Spetzler
Phoenix, Arizona

This study is very interesting, as it is one of the first to investigate the possible applications of tractography in surgery on the posterior fossa. Utilization of this type of data may provide information on the position of the cranial nerves.

The present study on 4 patients was performed with a 3-T magnetic resonance imaging (MRI) scanner, which acquired 3-mm-thick images. Tract reconstruction was obtained by defining regions of interest (ROIs) on the tensor volume, mainly identifying the cisternal portion of each nerve. However, it is not clear whether the results obtained were replicable in all 4 patients or whether there were any differences among the individual cases.

The authors state that the use of "ROI Select NOT" was necessary, but they do not specify how often this was needed for reconstruction of the longest tracts.

In our opinion, the most interesting finding is the representation of the course of cranial nerve III; both the brainstem intra-axial course and the cavernous and orbital portions are depicted in 3 dimensions. The study also shows the optic pathways from the retrobulbar portion to the calcarine cortex. However, the optical nerve, chiasm, and tracts are quite visible on many currently available conventional MRI sequences. Moreover, tractography of the intra-axial portion of the optical pathways has also been described. Regarding the other cranial nerves, those reconstructed by tractography are shown only in their cisternal portion, which is even better depicted with high-field, T2-weighted thin-slice imaging (eg, construction interference steady-state, fast imaging employing steady-state acquisition, and 3-dimensional [3D] fast spin echo).

On the whole, this is a very interesting and revelatory report, but we think that one should view with caution the conclusions of the authors, especially considering that these results were obtained with a continuing work-in-progress technique, diffusion tensor imaging; low-resolution images with a voxel size of approximately 2 × 2 × 3 mm (matrix size, 128 × 128; slice thickness, 3 mm; field of view size not specified), which approximates the diameter of many of the cranial nerves, were used. This article opens up a debate; let the debate begin!

Giuseppe Ricciardi
Albino Bricolo
Verona, Italy